

# Detecting Change in Vegetation Condition using High Resolution Digital Multispectral Imagery

Bradley Evans<sup>a,\*</sup>, Tom J. Lyons<sup>a</sup>, Paul A. Barber<sup>b</sup>, Christine Stone<sup>c</sup>, Giles Hardy<sup>b</sup>

<sup>a</sup> Centre of Excellence for Climate Change Woodland and Forest Health, School of Environmental Science, Murdoch University, 90 South Street, Murdoch, Western Australia, 6150 - b.evans@murdoch.edu.au, t.lyons@murdoch.edu.au

<sup>b</sup> Centre of Excellence for Climate Change Woodland and Forest Health, School of Biological Sciences, Murdoch University, 90 South Street, Murdoch, Western Australia, 6150 - p.barber@murdoch.edu.au, g.hardy@murdoch.edu.au

<sup>c</sup> Centre of Excellence for Climate Change Woodland and Forest Health, New South Wales Government Department of Industry and Investment, PO Box 100, Beecroft, NSW, Australia, 2125

**Abstract - Remote sensing of vegetation condition using high resolution digital multispectral imagery (DMSI) is an option for land managers interested in quantifying the distribution and extent of dieback in native forest. Crown condition is assessed as reference to the physical structure and foliage (i.e. density, transparency, extent and in-crown distribution) of a tree crown. At 20 sites in the Yalgorup National Park, Western Australia, a total of 80 (*Eucalyptus gomphocephala*) crowns are assessed both in-situ and using 2 acquisitions (2008 and 2010) of airborne DMSI. Each tree was assessed using four crown-condition indices: Crown Density, Foliage transparency, and the Crown Dieback Ratio and Epicormic Index. DMSI data is trained against canopy condition assessment data from 2008, crown condition is predicted using only spectral data. Comparison of DMSI derived Normalized Difference Vegetation Index (NDVI), Soil Adjusted Vegetation Index (SAVI) and a novel Red Edge Extrema Index (REEI) suggests the REEI is more suited to classification applications of this type.**

**Keywords:** dieback, crown condition, *Eucalyptus gomphocephala*, classification

## 1. INTRODUCTION

Eucalypt decline in Australia has increased over recent decades (Close et al., 2009; Horton et al., 2011). The visible decline symptom is defoliation, manifesting as a reduction in the overall density and distribution of foliage. In southwestern Australia, *Eucalyptus gomphocephala* (tuart) dominates the coastal dune systems of the Swan coastal plain (Boland et al., 2006). Since the early 1990's there has been concern for the spread of decline of tuart throughout parts of this region (see Figure 1) (Archibald et al., 2010; Close et al., 2009; Edwards, 2002; Horton et al., 2011).

Vegetation indices (VI) are used in remote sensing to relate biophysical attributes, such as vigor, photosynthetic activity and crown density to digital values of individual pixels. This is achieved by targeting specific regions in the spectrum and using multiband vegetation indices. The region in the spectrum between 690 nm and 740 nm is known as the 'red edge' (Curran et al., 1990) and is useful for characterizing chlorophyll content, (Pinar and Curran, 1996; Jago et al., 1999) density of chlorophyll in plant cells and crown density (Barry et al., 2008; Coops and Catling, 1997; Coops et al., 2002, 2003, 2004; Datt, 1998; Stone et al., 2001, 2003; Pietrzykowski et al., 2006).

Chlorophyll absorption in RED (i.e. the region from 600 nm to 700 nm) and NIR scattering (i.e. the region from 700 nm to 800 nm) results in a steep gradient, this is the 'red edge'. Dry eucalypt leaves scatter less NIR, so the slope of the 'red edge' is flatter. Studies have exploited the location, gradient and position of the red edge slope and related it to vegetation condition (Demetriades-Shah et al., 1990; Dawson and Curran, 1998).

The objectives of this study were to assess the accuracy of a number of DMSI derived VI for classifying the condition of tuart crowns in order to predict condition over time. DMSI Crown condition classifications were validated against ground based assessments using data available from 2008. Accordingly, the DMSI based classification was applied to multi-year (2008, 2010) time series to produce a change-over-time condition trajectory for individual trees.

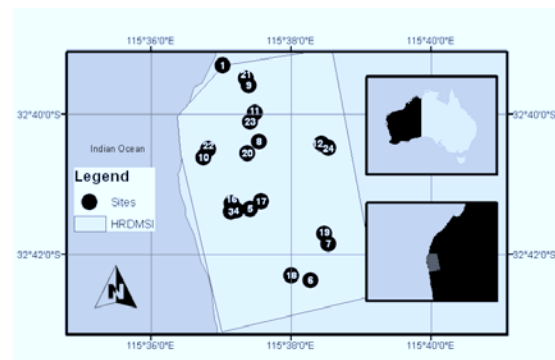


Figure 1: Map of the Yalgorup region showing the DMSI grid over the sites

## 2. METHODS

### 2.1. DMSI imagery and ground validation

The Yalgorup region (Figure 1) lies between 32° 38'0" S and 32° 44'0" S and 115° 36'0" E and 115° 40'0" E. Between 2005 and 2007, 20 sites were established to cover a range of vegetation cover trend classes from the 15-year (1990-2005) Land Monitor<sup>TM</sup> 25 m x 25 m multispectral imagery method described in Caccetta et al. (2000).

In July 2008, 80 trees were randomly selected across these sites and each crown was delineated using a differential GPS (dGPS)

with an accuracy of less than 1m. Using semi-quantitative assessment techniques, physical crown attributes (i) Crown Density (CD) and (ii) Foliage transparency (FT) indices (USDAFS, 2002) together with the (iii) Crown Dieback Ratio (CDR) and (iv) Epicormic Index (EI) (Kile et al., 1981; Wardlaw, 1989) were assessed for each crown. DMSI imagery was collected by SpecTerra Services Pty. Ltd. (Perth, Western Australia) using an airborne sensor developed specifically to map and monitor vegetation status at high spatial, spectral and radiometric sensitivities. DMSI was acquired at 0.5 m resolution in June 2008 and 2010 at similar solar angles under clear atmospheric conditions. The scenes were orthorectified as a sequence and pixel matched correcting for the sun angle of each flight.

The sensor acquires 12-bit digital data simultaneously in four 20 nm wide spectral channels in the visible and near-infrared regions of the electromagnetic spectrum using filters centred at BLUE (450 nm), GREEN (550 nm), RED (675 nm) and NIR (780 nm). Post flight processing of the data includes precise band to band registration and spectro-radiometric correction for bi-directional reflectance distribution function (BRDF) variations (SpecTerra Services Pty. Ltd). A 'like-value' calibration of the 2008 and 2010 DMSI data was conducted using a variant of the method described in Furby and Campbell (2001).

## 2.2. Vegetation Indices

The VI generated for this study are listed in Table 1 and replace NIR band with SpecTerra Services Ltd 780 nm ± 10 nm and any red band with 675 ± 10 nm. DMSI bands are significantly narrower than the broader bands used on satellite systems. For example, a Landsat Normalised Difference Vegetation Index (NDVI), which has been derived from various platforms, often uses broad bands > 50 nm (Deering and Rouse, 1975).

Table 1: Vegetation indices

Index	Equation	Adapted from
NDVI	$(780 \text{ nm} - 675 \text{ nm}) / (780 \text{ nm} + 675 \text{ nm})$	Rouse (1974); Deering and Rouse (1975); Huete et al. (2002)
REEI	$780 \text{ nm} / 675 \text{ nm}$	Sims and Gamon (2002); Gitelson and Merzlyak (1996)
SAVI	$(1+L)(790 \text{ nm} - 675 \text{ nm}) / (780 \text{ nm} + 675 \text{ nm}) + L$  Where; L is a canopy background factor accounting for 780 nm and 675 nm extinction through the canopy and L=0.5	Huete et al. (1994)

Narrow band pass filters, i.e. ±10 nm to ± 20 nm, sharpen the

contrast between RED and NIR by reducing noise. The novel Red Edge Extrema Index (REEI), shown in Table 1, expresses the contrast between RED and NIR as a simple ratio of the two and follows after broader band versions of the same concept by Sims and Gamon (2002); Gitelson and Merzlyak (1996).

The Soil Adjusted Vegetation Index (SAVI) used in this study, developed by Huete (1988), ignores the constraint of atmospheric correction because the DMSI was collected under low atmospheric vapour conditions. SAVI reduces soil brightness effects and eliminates the need to calibrate for various soil types (Huete, 1988; Huete et al., 1992, 1994; Karnieli et al., 2001). The default soil calibration coefficient is used in this study because the combination of high resolution data and the crown only focus eliminates the mixed pixel issues.

## 2.3. Condition classification

Figure 2 provides crown condition quintiles representing healthy (H) and declining crown condition classes (D) from healthy through to declining. Each quintile represents a 20% range indicated in its name i.e. H68 represents a crown of approximately 60-80% of its ideal (assumed to be a 100% foliated, vigorous specimen). Table 2 maps the classes to the ground based assessment parameters.

$$iFT = (100 - FT) \quad (1)$$

$$iCDR = (100 - CDR) \quad (2)$$

$$iEI = (100 - EI) \quad (3)$$

$$TCHI = CD + iFT + iCDR + iEI \quad (4)$$

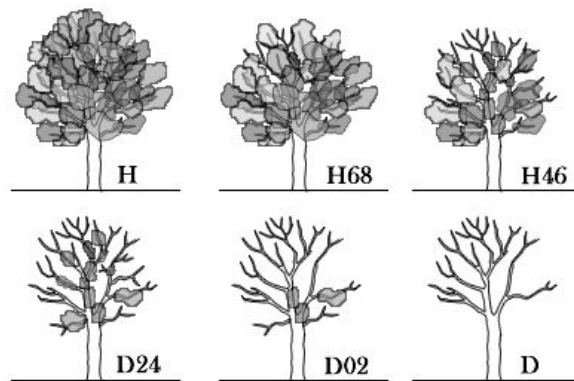


Figure 2: Tree condition classification key featuring 5 x 20% band groups covering 5 classes of healthy and declining crowns and a total mortality class (D).

Table 2: Mapping of NDVI, REEI, SAVI and TCHI to the tree condition classification

Class	NDVI	REEI	SAVI	TCHI
H	86-100	87-100	82-100	81-100
H68	65-85	72-86	65-81	61-80
H46	50-64	65-71	50-64	41-60
D24	21-50	41-64	21-50	21-40
D02	0-20	0-40	0-20	1-20

This crown condition classification scheme is designed for simplicity and adaptability with large margin for error, as compared to the prediction of a continuous variable, hence buffering both the limitations of the ground based assessments and the non-linearity of the VI. Ground based assessments are combined into a single continuous variable, the Total Crown Health Index (TCHI), shown in Equation 4. TCHI is an average of the sums of the inversely related canopy assessment parameters. Using the distribution of TCHI as a baseline, each VI distribution was empirically mapped into the condition class quintile breaks (refer Figure2) resulting in Table 2.

### 3. RESULTS

#### 3.1. DMSI Vegetation Indices

Comparison of VI distributions, using Figure 3, shows REEI to exhibit the most normalized distribution of the set and a close correlation between NDVI and SAVI. REEI is the least skewed (Tables 3 and 4) and has the lowest kurtosis. The skewness and kurtosis of both NDVI and SAVI are similar despite significant difference in the upper (UCL) and lower control limit (LCL) means (Tables 3 and 4). Both NDVI and SAVI, as normalized indices have some negative values. As is to be expected from a simple ratio, REEI has the highest range of all three across both years. Analysis of the mean, median and maximum peak of NDVI and SAVI (Tables 3 and 4 and Figure 3) show the classic saturation of VI near their upper limit. This feature is less in REEI, consistent with its more normalized distribution, skewness and kurtosis.

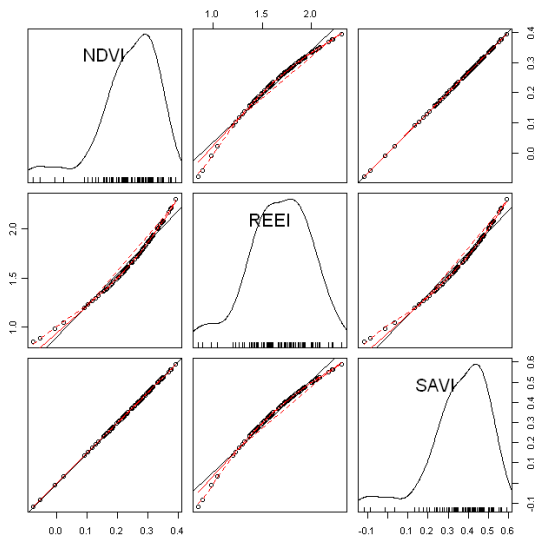


Figure 3: Covariate matrix of NDVI, REEI and SAVI derived from 80 mean quart-in-crown pixel values

#### 3.2. TCHI and crown classification

Figure 4 shows the difference in distribution of the crown classes between the TCHI and DMSI VI derived classifications. REEI over predicted the healthy classes with a variance range of  $\pm 2$  crowns yet performed well at estimating the declining classes  $\pm 1$ . NDVI performed better on the healthy classes  $\pm 1$  crowns, consistent with its saturation in the upper limit of its distribution, was under on D24 (-2) and over on D02 (+1). SAVI performed similar to NDVI in the declining classes yet was more varied than NDVI in the healthy classes (refer Figure 4). NDVI and REEI have a total of 6 point variance from the TCHI classification, SAVI 8.

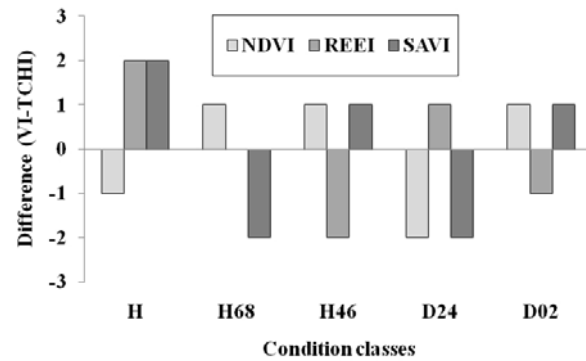


Figure 4: Difference between the TCHI of 80 quart and DMSI derived mean in-crown vegetation indices calculated for 2008

Table 3: Statistical summary of vegetation indices calculated for 2008

Statistic	NDVI	REEI	SAVI
Minimum	-0.079	0.854	-0.117
Maximum	0.394	2.301	0.589
1st Qu.	0.197	1.491	0.295
Mean	0.243	1.680	0.364
Median	0.261	1.708	0.391
3rd Qu.	0.308	1.889	0.460
Variance	0.009	0.092	0.020
Std Dev.	0.094	0.303	0.140
SE Mean	0.011	0.034	0.016
LCL Mean	0.223	1.613	0.331
UCL Mean	0.264	1.748	0.395
Skewness	-1.227	-0.459	-1.223
Kurtosis	2.087	0.190	2.075

Table 4: Statistical summary of vegetation indices calculated for 2010

Statistic	NDVI	REEI	SAVI
Minimum	-0.036	0.930	-0.054
Maximum	0.450	2.635	0.673
1st Qu.	0.209	1.530	0.313
Mean	0.274	1.809	0.409
Median	0.294	1.831	0.439
3rd Qu.	0.350	2.076	0.523
Variance	0.012	0.150	0.026
Std Dev.	0.108	0.387	0.162
SE Mean	0.012	0.043	0.018
LCL Mean	0.250	1.723	0.373
UCL Mean	0.298	1.896	0.445
Skewness	-0.914	-0.220	-0.911
Kurtosis	0.580	-0.320	0.574

### 3.3. Condition class change

Figure 5 shows the change in condition class between the two scenes, for each of the VI. Each performed surprisingly differently. REEI shows a net reduction in healthy crowns and an increase in declining crowns. This is consistent, albeit less intense in NDVI; however, SAVI shows a net growth trend for the health classes and extreme mean variance of  $\pm 10$  in the declining classes, confirming decline but suggesting it to be more severe than what NDVI and REEI indicate.

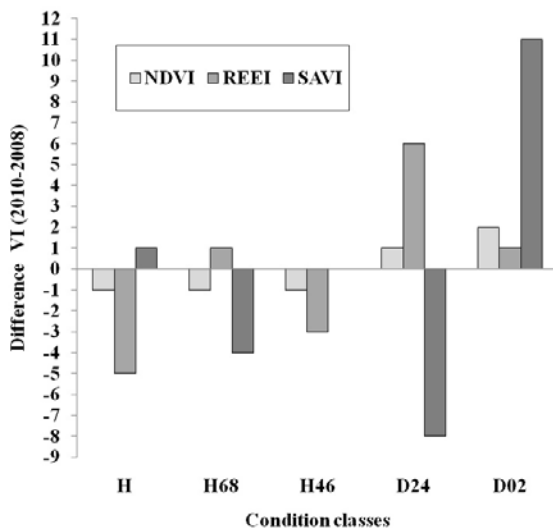


Figure 5: Change in crown condition classes from 2008 to 2010 using DMSI VI

## 4. DISCUSSION

There are numerous methodologies for assessing canopy density and foliage distribution and much work has already been done on validating these for eucalypts (Stone and Haywood, 2006). The recent work of Horton et al. (2011) found that CD and EI were the best performing indicators of crown condition in a review of Stone and Haywood (2006) and other work. Horton et al. (2011) also studied tuart in Yalgorup, from another patch of forest in the region. This approach of combining all four indices into a single, TCHI, attempts to account for structural and physiological differences in foliage throughout the crown.

The results suggest that simplifying high resolution DMSI data into target size objects (i.e. mean tree crown VI) reduces the impact of the salt and pepper and mixed pixel effects often found in lower resolution ( $> 10$  m) sensors (Yu et al., 2006). The salt and pepper effect is specific to high resolution sensors (1-10m) and disrupts classification routines attempting to compare neighboring pixels within a target object, for example a gap in a crown could result in a densely foliated branch next to a soil dominated pixel. The opposite, the mixed pixel effect results in a mixture of photosynthetic active and non-photosynthetic material and inevitably understory or ground cover where the larger pixel covers more than the target and combines gaps (Somers et al., 2010).

This combination of the object based classification and targeting RED and NIR bands results in strong classification performance despite saturation evident in both NDVI and SAVI. Furthermore, it is surprising that SAVI soil reduction parameter did not reduce the saturation effect. Whilst NDVI appeared more robust at predicting high green biomass crowns (i.e. H class) its overall performance, like SAVI, was less at crowns with decline when compared to REEI. Accordingly, the performance of the less saturated and more normally distributed REEI suggests it is more suited to this classification approach.

Given REEI's performance in this study, its larger and more normally distributed range, REEI lends itself to the application scene-scene image based visual change detection. That is, pixel rendering the difference between the REEI of two scenes to derive a difference image. Broadly speaking, large losses in REEI will indicate a reduction of green biomass whereas gains illustrate growth. Combined with this simple condition classification approach it is possible to map these gains and losses to condition with the aid of a species distribution map.

## 5. CONCLUSIONS

It is concluded that all three VI performed well and REEI appeared the best all round VI for condition classification using only DMSI. REEI featured the largest range of all three indices and this provided greater flexibility for quantile classification against health classes.

The VI and ground based assessment techniques presented provide land managers a means of assessing changes to individual crowns over time, making annual to seasonal change detection of tree decline possible at the individual tree scale. As

such it provides a framework for an ongoing monitoring that combines operationally proven, ground based assessments and DMSI.

## REFERENCES

- Archibald, R., Bradshaw, J., Bowen, B., Close, D., McCaw, L., Drake, P., Hardy, G., 2010. Understorey thinning and burning trials are needed in conservation reserves: The case of tuart (*eucalyptus gomphocephala* dc). *Ecological Management & Restoration* 11(2), 108–112.
- Barry, K., Stone, C., Mohammed, C., 2008. Crown-scale evaluation of spectral indices for defoliated and discoloured eucalypts. *International Journal of Remote Sensing* 29 (1), 47–69.
- Boland, D., Brooker, M., Chippendale, G., McDonald, M., Hall, N., Hyland, B., 2006. *Forest trees of Australia*. CSIRO.
- Caccetta, P., Allen, A., Watson, I., 2000. The land monitor project. RSPAA., Adelaide, pp. 97–107.
- Close, D., Davidson, N., Johnson, D., Abrams, M., Hart, S., Lunt, I., Archibald, R., Horton, B., Adams, M., 2009. Premature decline of eucalyptus and altered ecosystem processes in the absence of fire in some Australian forests. *The Botanical Review* 75, 191–202.
- Coops, N., Dury, S., Smith, M.-L., Martin, M., Ollinger, S., 2002. Comparison of green leaf eucalypt spectra using spectral decomposition. *Australian Journal of Botany* 50 (5), 567–576.
- Coops, N., Stone, C., Culvenor, D., Chisholm, L., 2004. Assessment of crown condition in eucalypt vegetation by remotely sensed optical indices. *Journal of Environmental Quality* 33 (3), 956–964.
- Coops, N., Stone, C., Culvenor, D., Chisholm, L., Merton, R., 2003. Chlorophyll content in eucalypt vegetation at the leaf and canopy scales as derived from high resolution spectral data. *Tree Physiology* 23 (1), 23–31.
- Coops, N.C., Catling, P.C., 1997. Predicting the complexity of habitat in forests from airborne videography for wildlife management. *International Journal of Remote Sensing* 18 (12), 2677–2682.
- Curran, P., Dungan, J., Gholz, H., 1990. Exploring the relationship between reflectance red edge and chlorophyll content in slash pine. *Tree Physiology* 7, 33–48.
- Datt, B., 1998. Remote sensing of chlorophyll a, chlorophyll b, chlorophylla+b, and total carotenoid content in eucalyptus leaves. *Remote Sensing of Environment* 66 (2), 111–121.
- Dawson, T., Curran, P., 1998. Technical note a new technique for interpolating the reflectance red edge position. *International Journal of Remote Sensing* 19 (11), 2133–2139.
- Deering, D., Rouse, J., 1975. Measuring ‘forage production’ of grazing units from landsat mss data. 1169–1178.
- Demetriades-Shah, T., Steven, M., Clark, J., 1990. High resolution derivative spectra in remote sensing. *Remote Sensing of Environment* 33 (1), 55–64.
- Edwards, T., 2002. Environmental correlates and associations of tuart decline. Ph.D. thesis, M. Sc. Thesis, Edith Cowan University, Perth, Western Australia.
- Furby, S., Campbell, N., 2001. Calibrating images from different dates to ‘like-value’ digital counts. *Remote Sensing of Environment* 77 (2), 186–196.
- Gitelson, A., Merzlyak, M., 1996. Signature analysis of leaf reflectance spectra: algorithm development for remote sensing of chlorophyll. *Journal of Plant Physiology* 148 (3), 494–500.
- Horton, B. M., Close, D. C., Wardlaw, T. J., Davidson, N. J., 2011. Crown condition assessment: An accurate, precise and efficient method with broad applicability to eucalyptus. *Austral Ecology*. (in press)
- Huete, A., Hua, G., Qi, J., Chehbouni, A., Van Leeuwen, W., 1992. Normalization of multidirectional red and nir reflectances with the savi. *Remote Sensing of Environment* 41 (2-3), 143–154.
- Huete, A., Justice, C., Liu, H., 1994. Development of vegetation and soil indices for modis-eos. *Remote Sensing of Environment* 49 (3), 224–234.
- Huete, A.R., 1988. A soil-adjusted vegetation index (savi). *Remote Sensing of Environment* 25 (3), 295–309.
- Jago, R., Cutler, M., Curran, P., 1999. Estimating canopy chlorophyll concentration from field and airborne spectra. *Remote Sensing of Environment* 68 (3), 217–224.
- Karnieli, A., Kaufman, Y., Remer, L., Wald, A., 2001. Afri-aerosol free vegetation index. *Remote Sensing of Environment* 77 (1), 10–21.
- Kile, G., Turnbull, C., Podger, F., 1981. Effect of regrowth dieback on some properties of eucalyptus obliqua trees. *Australian Forest Research* 11, 55–62.
- Pietrzykowski, E., Stone, C., Pinkard, E., Mohammed, C., 2006. Effects of mycosphaerella leaf disease on the spectral reflectance properties of juvenile eucalyptus globulus foliage. *Forest Pathology* 36 (5), 334–348.
- Pinar, A., Curran, P., 1996. Technical note grass chlorophyll and the reflectance red edge. *International Journal of Remote Sensing* 17 (2), 351–357.
- Sims, D., Gamon, J., 2002. Relationships between leaf pigment content and spectral reflectance across a wide range of species, leaf structures and developmental stages. *Remote Sensing of Environment* 81 (2-3), 337–354.
- Somers, B., Verbesselt, J., Ampe, E.M., Sims, N., Verstraeten, W.W., Coppin, P., 2010. Spectral mixture analysis to monitor defoliation in mixed-aged eucalyptus globulus Labill plantations in southern Australia using landsat 5-tm and eo-1hyperion data. *International Journal of Applied Earth Observation and Geoinformation* 12 (4), 270–277.
- Stone, C., Chisholm, L., Coops, N., 2001. Spectral reflectance characteristics of eucalypt foliage damaged by insects. *Australian Journal of Botany* 49 (6), 687–698.
- Stone, C., Haywood, A., 2006. Assessing canopy health of native eucalypt forests. *Ecological Management & Restoration* 7(s1), S24–S30.
- Stone, C., Wardlaw, T., Floyd, R., Carnegie, A., Wylie, R., de Little, D., 2003. Harmonisation of methods for the assessment and reporting of forest health in Australia starting point. *Australian Forestry* 66 (4), 233–246.
- USDAFS, 2002. *Forest inventory and analysis: National core field guide, 1: Field data collection procedures for phase2plots, version 1.6*.
- Wardlaw, T., 1989. Management of Tasmanian forests affected by regrowth dieback. *New Zealand Journal of Forest Science* 19, 265–276.
- Yu, Q., Gong, P., Clinton, N., Biging, G., Kelly, M., Schirokauer, D., 2006. Object-based detailed vegetation classification with airborne high spatial resolution remote sensing imagery. *Photogrammetric Engineering and Remote Sensing* 72 (7), 799.

## ACKNOWLEDGEMENTS

We thank SpecTerra Services Ltd. for their substantial support in the provision of the orthorectified digital multispectral imagery utilised for this study.